Electroosmotic Microfluidic Flows with Random Zeta Potential

James P. Gleeson

National Microelectronics Research Centre
and Department of Applied Mathematics,
University College Cork, Ireland
Email: j.gleeson@ucc.ie

ABSTRACT

Average electroosmotic flows in the presence of axially-varying zeta potentials are shown to be plug-like, with variances which depend on radial position across the capillary. Consequences for the dispersion of samples are examined theoretically and through numerical simulation.

Keywords: electroosmosis, zeta potential, turbulent diffusion

1 INTRODUCTION

Micro total analysis systems (μTAS) and other microfluidic systems increasingly rely on electrokinetic mechanisms for fluid transport. Electroosmotic flow, for example, arises in the presence of an electric double layer at the solid-liquid interface which is due to attraction between bound surface charges and ions in the fluid [1]. The application of an axial electric field E induces a sheath flow with velocity proportional to $E\zeta$, where ζ is the (constant) zeta potential of the wall surface charges. In the limit of thin electric double layer, the viscous drag of the sheath on the fluid results in a low Reynolds number flow with a constant velocity profile across the channel. This "plug-like" flow contrasts with the parabolic profile seen in flows driven by external pressure gradients.

Recent advances in experimental flow imaging for microchannels and capillaries have enabled the plug-like electrokinetic and parabolic pressure-driven flows to be visualized, measured and compared to numerical simulation [2], [3]. Surprisingly, it was found that some electroosmotic flows exhibit pronounced parabolic profiles instead of the expected plug-like form. Careful examination of the possible causes of this anomaly led Molho et al. [3] to propose the existence of pressure gradients induced by variations in the zeta potential along the length of the channel. They examined the effects of widely-spaced step changes in the zeta potential and verified experimentally [4] that the resulting flows have parabolic profiles.

In this paper we generalize the theoretical approach of [3], [4] to consider more realistic variations in the zeta potential. We take the zeta potential to be a function which varies randomly along the length of the capillary, with known average (mean) value $\bar{\zeta}$, variance σ^2, and correlation length l. The variance measures the extent of deviations of the actual ζ value from its mean $\bar{\zeta}$. Employing a Fourier transform solution [5], [6] for flow in cylindrical capillaries, we calculate the average ("expected") flow velocity and its variance. The average flow is found to be a plug-like flow, with velocity proportional to $E\bar{\zeta}$, as previously found in [4] and [6] for simple zeta defects. However, the variance of the axial velocity is shown to depend on radial position within the capillary, and exhibits a parabolic or near-parabolic profile, depending upon the variance σ^2 and correlation length l of the zeta potential. It is proposed that this dependence may be used to experimentally infer the characteristics of the surface zeta potential from measurements of the fluid velocity.

The non-zero variance of the axial and radial velocity components causes dispersion of an initially compact sample as it is transported through the channel. The nature of this dispersion is similar to (but distinct from) that due to molecular diffusion, and it may be modelled by defining an effective diffusion coefficient as is commonly done for turbulent transport [7], [8]. The effects of this dispersion are examined analytically and compared to numerical simulations.

2 FLOW IN A CAPILLARY

The axisymmetric motion of a fluid in a cylindrical capillary under the influence of an axially-varying zeta potential $\zeta(z)$ may be described by the solution of the Stokes equations with slip boundary conditions. Implicit assumptions are that the Reynolds number is very small compared to unity ("slow flow") and the Deybe length is much less than the capillary radius (i.e. thin electric double layer). The axis of the capillary is oriented in the z direction; r denotes the radial distance from the axis. The general solution may be written in terms of the Fourier transforms of the radial and axial velocities and pressure, see for example [5], [6]. In particular, the axial velocity transform is

$$\hat{v}_z(r,k) = \hat{G}(r,k)E\hat{\zeta}(k), \qquad (1)$$

for

$$\hat{G}(r,k) = \frac{I_0(kr)}{I_0(k)} + \frac{I_1(k)}{I_0(k)} \frac{k^2 r I_1(kr) I_0(k) - k^2 I_1(k) I_0(kr)}{k^2 I_1(k)^2 - k^2 I_0(k)^2 + 2k I_1(k) I_0(k)},$$

where the hats denote Fourier transforms in the axial direction, with inverses of the form

$$v_z(r,z) = \int_{-\infty}^{\infty} e^{ikz} \hat{v}_z(r,k) dk, \tag{2}$$

and E is the imposed (constant) electric field. Here I_0 and I_1 are modified Bessel functions of the first kind and lengths are nondimensionalized by the capillary radius. In the following we consider $\zeta(z)$ as a random function of position with given mean, variance and correlation length, and use (1) to infer statistical information about the axial velocity v_z.

3 THEORETICAL RESULTS

Overbars will denote averages over multiple measurements (or "realizations"). Multiple measurements may be on different capillaries of similar manufacture, or at well-spaced intervals along a single capillary. Note that this averaging over realizations is not the same as other averaging procedures commonly used, such as averaging over the cross-section of the capillary [7].

In order to quantify the dependence of the velocity variance on the zeta potential, we first consider the statistics of the latter. Assuming a homogeneous Gaussian random process, the statistical characteristics of the zeta potential are its mean $\overline{\zeta}$ and correlation function R. The correlation function is defined by

$$\overline{\zeta(z)\zeta(z')} - \overline{\zeta}^2 = \sigma^2 R(z - z'), \tag{3}$$

where σ^2 is the variance of the zeta potential and $R(0) = 1$. The function R decays to zero as its argument increases; a common form assumed for R is

$$R(z) = \exp(-\frac{z^2}{2l^2}), \tag{4}$$

with l being the length scale over which the random function is strongly correlated.

Since the velocity depends on the random zeta potential, it too is a random function. From (1), it is easy to show that the average axial velocity is given by

$$\overline{v_z} = E\overline{\zeta}, \tag{5}$$

and this average does not depend on z or r, i.e. *the mean flow is plug-like*. However, the measured value of the velocity will vary about this average, so we introduce the velocity variance $\overline{(v_z - \overline{v_z})^2}$. Assuming the correlation of the zeta potential is given by (3), it is straightforward to show that the variance of the axial velocity is given by the integral

$$\overline{(v_z - \overline{v_z})^2} = E^2\sigma^2 \int_{-\infty}^{\infty} \hat{G}(r,k)^2 \hat{R}(k) dk = E^2\sigma^2 f(r) \tag{6}$$

Note that this integral depends on r, i.e. *the amount of variation of v_z about its mean depends on the radial measurement position.* Figure 1 shows the nondimensional function

$$f(r) = \int_{-\infty}^{\infty} \hat{G}(r,k)^2 \hat{R}(k) dk \tag{7}$$

calculated using the correlation function (4). The function $f(r)$ is evaluated by numerical integration of (7) at each value of r. The variations are generally largest in the middle and at the sides of the capillary, with a minimum near $r = 1/\sqrt{2}$. Also plotted for comparison is the parabolic-squared function $(1 - 2r^2)^2$, which is approached by $f(r)$ in the limit $l \to \infty$. It is clear that the value of $f(r)$, and so of the velocity variance, depends strongly on the statistical characteristics σ^2 and l of the zeta potential, and we propose that measurements of velocity variance at various radial positions be used to estimate σ^2 and l. With this application in mind, a table of values of $f(r)$ for various r and l is provided in Table 1.

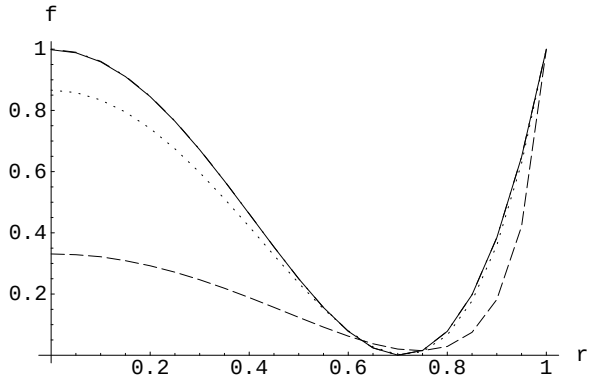

Figure 1: The function $f(r)$ for various values of the correlation length l: $l = 10$ solid; $l = 1$ dotted; $l = 0.2$ dashed. The comparison function $(1 - 2r^2)^2$ is indistinguishable from the solid line.

4 NUMERICAL SIMULATIONS

We have established that the variance of the axial velocity v_z depends on r. The effect of this variance is measurable when passive tracers are added to the fluid flows, e.g. dye markers. Consider a portion of the fluid which is marked with tracers. These tracers follow the

Table 1: Values of $f(r)$ for various r and l.

	$r=0$	$r=0.25$	$r=0.5$
$l=0.1$	0.173	0.143	0.069
$l=0.2$	0.331	0.271	0.124
$l=0.3$	0.465	0.377	0.162
$l=0.4$	0.573	0.460	0.187
$l=0.5$	0.657	0.524	0.204
$l=1$	0.866	0.674	0.236
$l=5$	0.993	0.761	0.249
$l=10$	0.998	0.765	0.250

fluid exactly (no molecular diffusion), so the equations of motion are

$$\begin{aligned} \frac{dr_p}{dt} &= v_r(r_p, z_p) \\ \frac{dz_p}{dt} &= v_z(r_p, z_p), \end{aligned} \tag{8}$$

for a tracer particle with position $(r_p(t), z_p(t))$. If many such tracers are released and followed for a finite time, the average (over multiple experiments) of their final positions is related to the statistical characteristics of the fluid velocity. In our numerical simulations, we take a number of particles released at various radial positions across the capillary, all with $z = 0$. The final positions of these particles will depend on the random fluid velocity, which in turn depends on the zeta potential. Random Gaussian zeta potentials were created following [8], [9]—in each realization the zeta potential is given by the sum over N_m random Fourier modes:

$$\zeta(z) = \overline{\zeta} + \frac{1}{\sqrt{N_m}} \sum_{n=1}^{N_m} A_n \cos(k_n z) + B_n \sin(k_n z), \tag{9}$$

where k_n, A_n and B_n are taken from independent Gaussian distributions with variances l^{-2}, σ^2 and σ^2 respectively. Lengths and times are nondimensionalized so that the capillary radius is one, and the average velocity $\overline{v_z} = E\overline{\zeta}$ is unity. The axial velocity is then constructed by using the inverse of (1) with v_r found similarly, and a predictor-corrector method [8] is used to numerically solve (8) for the particles' positions at a nondimensional final time of $t = 2$. This is considered to be "short-time" advection, as the average final distance $\overline{z_p(t=2)} = 2$ is much smaller than the correlation length $l = 10$ of the zeta potential. The variance across the capillary is plotted in Figure 2; in Figure 3 we plot the average concentration profile (representing the probability distribution of the particle positions over many realizations) The mean position of the particles at $t = 2$ is $\overline{z_p} = \overline{v_z}t = 2$ as expected. According to the theory of turbulent diffusion [10], the variance of the advected particles over this short time can be related to the variance of the velocity

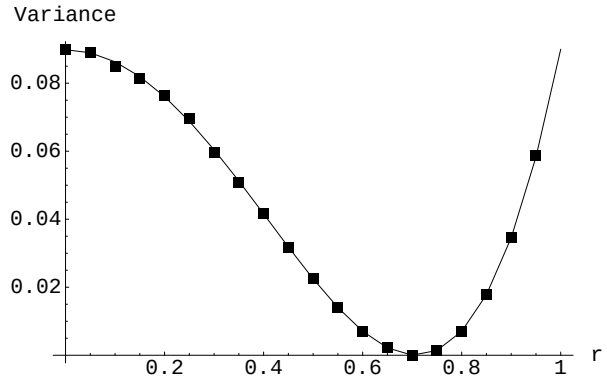

Figure 2: The function $E^2\sigma^2 f(r)t^2$ (line) and the numerical simulation results (symbols) for variance of advected particles. Parameters are $\overline{\zeta} = 1$, $E = 1$, $l = 10$, $\sigma = 0.15$, $N = 25000$, $N_m = 1$.

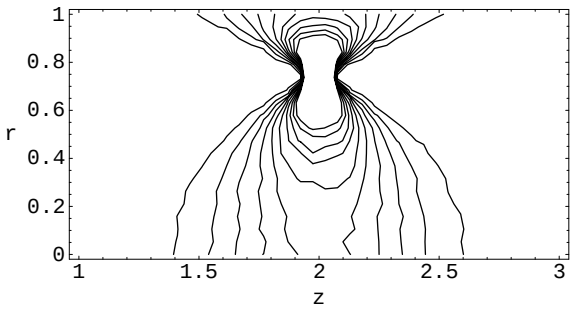

Figure 3: Numerical concentration profile contours at $t = 2$. Parameters are as in Figure 2.

by

$$\begin{aligned} \overline{(z_p - \overline{z_p})^2} &= \overline{(v_z - \overline{v_z})^2} t^2 \\ &= E^2\sigma^2 f(r) t^2, \end{aligned} \tag{10}$$

provided that σ is small enough so that the radial position of each particle does not vary too much over the time t. Our numerical results show a clear dependence of the form (10), and indeed the concentration profile is well approximated by the normal Gaussian form

$$P(r,z) = \frac{1}{\sqrt{2\pi\overline{(z_p - \overline{z_p})^2}}} \exp\left[-\frac{(z - \overline{v_z}t)^2}{2\overline{(z_p - \overline{z_p})^2}} \right], \tag{11}$$

as shown in Figure 4.

5 LONG-TIME SIMULATIONS

The average effects of tracer advection can be successfully described by turbulent diffusion theory for short times, as demonstrated in the last section. However, the effects of dispersion over longer times is clearly important, especially for realistic comparison with experiments. As a first step in this direction, we consider

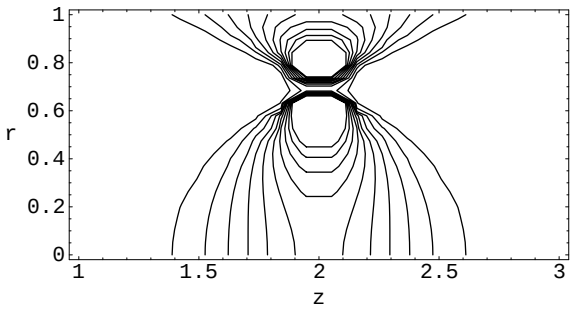

Figure 4: Theoretical concentration profile contours at $t = 2$ given by (11).

the solution of (8) for particles initially on the capillary axis at $r_p = 0$. Because of the symmetry of the problem, particles on the axis must remain there, so (8) is reduced to a one-dimensional problem for the axial position z_p. In the simple case $N_m = 1$ this may be solved exactly in each realization, allowing us to consider the results of long time ($t \gg l/\overline{v_z}$) advection. Results (not shown) yield a mean position $\overline{z_p}$ increasing approximately as $\overline{v_z}t$ as before, even up to $t = 80$. The t^2 shape of the variance given by (10), however, is only valid for $t < 15$. Thereafter the diffusion may be described by analogy with the classical Brownian motion theory, which predicts a variance proportional to t for large t. The coefficient of proportionality is termed the "effective diffusivity", and can be calculated for small σ using the methods of e.g. [8] to give

$$\overline{(z_p - \overline{z_p})^2} = \frac{E^2\sigma^2 z_*}{\overline{v_z}}t,$$

where z_* is the correlation length defined by

$$z_* = \int_0^\infty R(z)dz.$$

Accordingly, in Figure 5 we plot a straight line with slope $E\sigma^2 z_*/\overline{\zeta}$, which is seen to match the slope of the numerical variance quite well. Further work on the application of these results to long-time dispersion across the capillary is continuing.

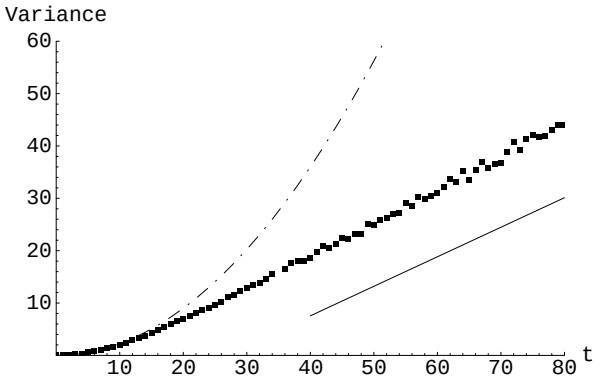

Figure 5: Long-time numerical variance (symbols) at $r = 0$, with the function $E^2\sigma^2t^2$ (dashed). The solid line has slope $E^2\sigma^2 z_*/\overline{v_z}$. Parameters are $\overline{\zeta} = 1$, $E = 1$, $l = 10$, $\sigma = 0.15$, $N = 10000$, $N_m = 1$.

REFERENCES

[1] Rice C.L. and Whitehead R. "Electrokinetic flow in a narrow cylindrical capillary," *J. Phys. Chem.* **69**, 4017 (1965)

[2] Paul P.H., Garguilo M.G. and Rakestraw D.J. "Imaging of pressure- and electrokinetically driven flows through open capillaries," *Anal. Chem.* **70**, 2459 (1998)

[3] Molho J.I. et al. "Fluid transport mechanisms in microfluidic devices," *MEMS, 1998 ASME International Mechanical Engineering Congress and Exposition* (1998)

[4] Herr A.E., Molho J.I., Santiago J.G., Mungal M.G. and Kenny T.W. "Electroosmotic capillary flow with nonuniform zeta potential," *Anal. Chem.* **72**, 1053 (2000)

[5] Long D., Stone H.A. and Ajdari A. "Electroosmotic flows created by surface defects in capillary electrophoresis," *J. Colloid Interface Sci.* **212**, 338 (1999)

[6] Anderson J.L. and Idol W.K. "Electroosmosis through pores with nonuniformly charged walls," *Chem. Eng. Commun.* **38**, 93 (1985)

[7] Taylor G.I. "The dispersion of matter in turbulent flow through a pipe," *Proc. R. Soc. London, Ser. A* **223**, 446 (1954)

[8] Gleeson J.P. "A closure method for random advection of a passive scalar," *Phys. Fluids* **12**, 1472 (2000)

[9] Kraichnan R.H. "Diffusion by a random velocity field," *Phys. Fluids* **13**, 22 (1970)

[10] McComb W.D. *The Physics of Fluid Turbulence*, Oxford University Press (1990)